IEEE Access
Multidisciplinary | Rapid Review | Open Access Journal

Received February 27, 2019, accepted March 4, 2019, date of publication March 8, 2019, date of current version April 8, 2019.

Digital Object Identifier 10.1109/ACCESS.2019.2903934

Path Tracking of Wheeled Mobile Robots Based on Dynamic Prediction Model

GUOXING BAI[1], LI LIU[1], YU MENG[1,2], WEIDONG LUO[1], QING GU[1], AND JUNPENG WANG[1]
[1]School of Mechanical Engineering, University of Science and Technology Beijing, Beijing 100083, China
[2]Institute of Artificial Intelligence, University of Science and Technology Beijing, Beijing 100083, China

Corresponding author: Yu Meng (myu@ustb.edu.cn)

This work was supported in part by the National Key Research and Development Program of China under Grant 2018YFC0604403 and Grant 2016YFC0802905, in part by the National High Technology Research and Development Program of China (863 Program) under Grant 2011AA060408, and in part by the Fundamental Research Funds for the Central Universities under Grant FRF-TP-17-010A2.

ABSTRACT In the field of path tracking control for wheeled mobile robots, researchers generally believe that the motion of robots meets non-holonomic constraints. However, the robot may sideslip by centrifugal force when it is steering. This kind of slip is usually uncontrollable and dangerous. In order to prevent sideslip and improve the performance of path tracking control, we propose a controller based on tire mechanics. Moreover, the new controller is based on the model predictive control, and this control method has proven to be suitable for path tracking of wheeled mobile robots. The proposed controller was verified by simulation and compared with a model predictive controller based on kinematics (non-holonomic constraints). As for the simulation results, the maximum values of displacement error, heading error, lateral velocity, and slip angle of the dynamic-based model predictive controller are 0.2086 m, 0.1609 rad, 0.1546 m/s, and 0.0576 rad, respectively. Compared with the kinematics-based model predictive controller, the maximum values of the above-mentioned parameters of the dynamic-based controller reduce by 86.55%, 72.25%, 96.30%, and 90.02%, respectively. The above-mentioned results show that the proposed controller can effectively improve the accuracy of path tracking control and avoid sideslip.

INDEX TERMS Wheeled mobile robot, path tracking, path following, model predictive control, dynamic model.

I. INTRODUCTION

Wheeled mobile robots are widely applied in interstellar exploration, military, manufacturing, cargo transportation and other industries [1]–[3]. Usually, a properly functioning wheeled mobile robot is equipped with a navigation system, and the path tracking is the key part of the navigation. The task of the path tracking is to control the wheeled mobile robot tracking the given path as close as possible.

A. MOTIVATIONS

For cargo transportation, the operational efficiency of the wheeled mobile robot as shown in Fig.1, has a significant effect on economy. And the higher driving velocity will make the wheeled mobile robot run more efficiently. However, Sidek and Sarkar [4] pointed out that wheeled mobile robots may skid when steering at high driving velocity, and the sideslip not only impacts the accuracy of the path tracking control, but also can cause danger. Therefore, the purpose of this work is to propose a new controller. This controller should enable the mobile robot to track the given path

FIGURE 1. Wheeled mobile robot.

The associate editor coordinating the review of this manuscript and approving it for publication was Ning Sun.

accurately at the highest driving velocity as much as possible, and it should reduce sideslip of the wheeled mobile robot.

B. RELATED WORKS

At present, there are many published papers on path tracking control for wheeled mobile robots.

For traditional control methods, based on feedback linearization control, path tracking controllers for wheeled mobile robots are proposed respectively in [4]–[6]. Reference [7] proposes a pure pursuit controller for the path tracking of mobile robots. Reference [8] presents a back-stepping controller.

For intelligent control methods, neural network control, fuzzy control, sliding mode control and adaptive control also have many research results in this field. Reference [9] proposes a reinforcement learning controller, [10] proposes a fuzzy controller, [11] proposes a fuzzy neural network controller, [12] and [13] propose sliding mode controllers, [14] proposes an adaptive controller, and [15] proposes an adaptive sliding mode controller.

Another common intelligent control algorithm in path tracking control of wheeled mobile robots is model predictive control (MPC). References [16]–[23] propose some MPC-based path tracking controllers, and the effect of these controllers proves the point raised in [24] that the biggest advantage of MPC over other control methods is that the MPC can take into consideration the constraints of wheeled mobile robots explicitly.

We agree with the views of [16]–[24] for MPC, but the sideslip which was pointed out in [4] cannot be ignored. References [16]–[23] assume that the wheeled mobile robot meets the non-holonomic constraints and ignores the problem of sideslip, and the MPC controllers are based on the kinematics prediction model in these researches. Therefore, we think it is necessary to propose a model predictive controller that takes sideslip into account to improve the performance of path tracking control of wheeled mobile robots.

C. CONTRIBUTIONS

In order to improve the accuracy of the MPC-based path tracking and reduce the sideslip of wheeled mobile robots, the controller based on the nonlinear dynamic prediction model is proposed in this paper. Our work makes the following contributions. Firstly, based on rigid body mechanics and tire mechanics, the dynamic model of the wheeled mobile robot considering sideslip is established. Secondly, the prediction model is derived based on the dynamic model, and the design of the MPC controller is completed. Finally, by adding the lateral velocity penalty term and decoupling, the MPC controller based on the dynamic prediction model is further improved to reduce tracking error and sideslip.

The rest of this paper is arranged as follows. Section II introduces the dynamic model and the constraints of the wheeled mobile robot. In section III, the MPC controller based on the dynamic model is designed and verified. In section IV, the MPC controller is further improved and verified. In addition, there is a brief conclusion in the last section.

II. DYNAMIC MODEL AND CONSTRAINTS

The wheeled mobile robot shown in Fig.1 is equipped with four wheels, of which the front and rear are universal wheels, and the left and right are driving wheels, as shown in Fig.2.

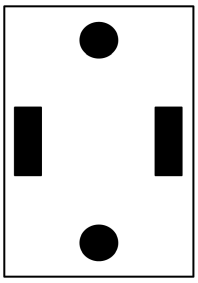

FIGURE 2. Wheels layout of the wheeled mobile robot.

A. DYNAMIC MODEL

Referring to [25]–[28], the dynamic model of the wheeled mobile robot is established by the Newton-Euler method.

Since the universal wheel is only subjected to the resistance opposite to the direction of the linear velocity, and the front and rear universal wheels are symmetrical, the influence of the front and rear wheels on the robot is small. Therefore, the force on the wheeled mobile robot can be simplified as shown in Fig.3. The definition of variables in Fig.3 is shown in Table 1.

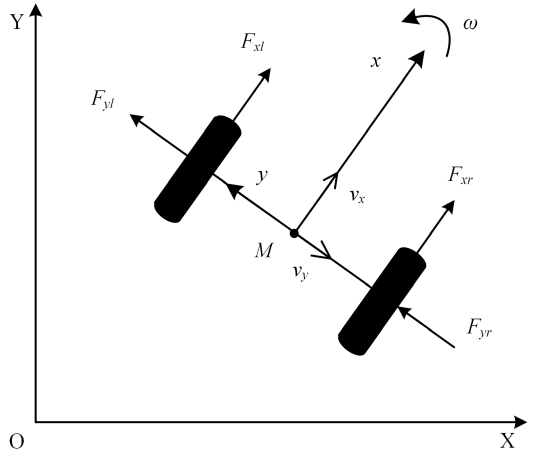

FIGURE 3. Force on the wheeled mobile robot.

According to the relationship between velocities and coordinates, the following formulas can be obtained:

$$\begin{cases} \dot{X} = v_x \cos\theta - v_y \sin\theta \\ \dot{Y} = v_x \sin\theta + v_y \cos\theta \end{cases} \tag{1}$$

For controlling the longitudinal velocity and the heading angle speed by the driving force, [29] has put forward a good controller. So in this paper, it is assumed that v_x and ω can be controlled directly.

TABLE 1. Variable in Fig.3.

Symbol	Quantity	SI
XOY	world coordinate system	m
xoy	relative coordinate system	m
o	center of gravity	
v_x	longitudinal velocity	m/s
v_y	lateral velocity	m/s
ω	heading angle speed	rad/s
θ	heading angle	rad
F_{xl}	driving force of the left wheel	N
F_{yl}	lateral force of the left wheel	N
F_{xr}	driving force of the right wheel	N
F_{yr}	lateral force of the right wheel	N

For the lateral velocity, the following equation can be obtained in the y-direction:

$$\dot{v}_y = \frac{1}{m}F_y - v_x\omega \tag{2}$$

where m is the quality of the wheeled mobile robot, and:

$$F_y = F_{yr} + F_{yl} \tag{3}$$

According to the Magic Formula [29]–[33] in the Appendix, the lateral force is a function of the slip angle:

$$F_y = 2f_y(\alpha) \tag{4}$$

where the slip angle is defined as:

$$\alpha = \arctan\frac{v_y}{v_x} \tag{5}$$

Therefore, the lateral velocity is a function of longitudinal velocity and heading angular velocity:

$$\dot{v}_y = f(v_x, \omega) \tag{6}$$

Combining $\dot{\theta} = \omega$, the dynamic model of wheeled mobile robots considering the sideslip can be written as:

$$\begin{cases} \dot{X} = v_x\cos\theta - v_y\sin\theta \\ \dot{Y} = v_x\sin\theta + v_y\cos\theta \\ \dot{\theta} = \omega \\ \dot{v}_y = f(v_x, \omega) \end{cases} \tag{7}$$

B. CONSTRAINTS

Since the driving force of the wheeled mobile robot is within a certain range, there are some constraints to the changing of the longitudinal velocity and the heading angle speed.

According to Newton's Second Law of Motion-Force and Acceleration, the following formulas can be obtained:

$$\begin{cases} \dot{v}_x = (F_{xr} + F_{xl})/m \\ \dot{\omega} = (F_{xr} - F_{xl})\, b/2I_z \end{cases} \tag{8}$$

where I_z is the moment of inertia, b is the width of the wheeled mobile robot.

Since the sampling interval T is small enough, the longitudinal velocity increment and angle speed increment can be defined as follows:

$$\begin{cases} \Delta v = T\dot{v}_x \\ \Delta\omega = T\dot{\omega} \end{cases} \tag{9}$$

Therefore, the constraints of the wheeled mobile robot are:

$$\begin{cases} TF_{x\min}/m \le \Delta v \le TF_{x\max}/m \\ TM_{\min}/I_z \le \Delta\omega \le TM_{\max}/I_z \end{cases} \tag{10}$$

where:

$$\begin{cases} F_{x\min} = F_{xr\min} + F_{xl\min} \\ F_{x\max} = F_{xr\max} + F_{xl\max} \\ M_{\min} = (F_{xr\min} - F_{xl\max})\, b/2 \\ M_{\max} = (F_{xr\max} - F_{xl\min})\, b/2 \end{cases} \tag{11}$$

Generally, programs such as emergency stop have higher priority than path tracking control, so the range of constraints in path tracking control can be narrowed to make path tracking more smoothly. In this paper, the constraints of the wheeled mobile robot are set as:

$$\begin{cases} TF_{x\min}/2m \le \Delta v \le TF_{x\max}/2m \\ TM_{\min}/2I_z \le \Delta\omega \le TM_{\max}/2I_z \end{cases} \tag{12}$$

Substituting $T = 0.05$s, parameters of the wheeled mobile robot, including $m = 1200$kg and $I_z = 400\text{kg}\cdot\text{m}^2$, and parameters obtained by the Magic Formula in the Appendix, including $F_{x\max} = 8.8$kN and $F_{x\min} = -8.8$kN, into (11) and (12), the values of constraints are set as:

$$\begin{cases} -0.1836\text{m/s} < \Delta v < 0.1836\text{m/s} \\ -0.33\text{rad/s} < \Delta\omega < 0.33\text{rad/s} \end{cases} \tag{13}$$

III. DESIGN AND SIMULATION OF MPC CONTROLLER

A. DESIGN

The basic part of the MPC controller is the prediction model. In this paper, the prediction model is derived from the dynamic model (7).

The dynamic model (7) is abbreviated as:

$$\dot{\mathbf{x}} = f_d(\mathbf{x}, \mathbf{u}) \tag{14}$$

where:

$$\begin{cases} \mathbf{x} = \begin{bmatrix} X & Y & \theta & v_y \end{bmatrix}^T \\ \mathbf{u} = \begin{bmatrix} v_x & \omega \end{bmatrix}^T \end{cases} \tag{15}$$

Since T is very small, (14) can be discretized into:

$$\mathbf{x}(i+1|t) = \mathbf{x}(i|t) + Tf_d(\mathbf{x}(i|t), \mathbf{u}(i|t)) \tag{16}$$

Then, the errors between the wheeled mobile robot and the given path can be obtained:

$$\mathbf{e}(i|t) = \mathbf{x}(i|t) - \mathbf{x}_{ref}(i|t)$$

$$\begin{aligned}\vdots\\ \mathbf{e}\left(N_p|t\right) &= \mathbf{x}\left(N_p|t\right)\\ &\quad -\mathbf{x}_{ref}\left(N_p|t\right)\end{aligned} \tag{17}$$

where N_p is the prediction horizon, and $\mathbf{x}_{ref}$ is the reference point on the given path.

After obtaining the prediction model, the next key in designing the MPC controller is the optimization function.

For the path tracking control of wheeled mobile robots, the most important optimization goal is to reduce the error, so the first penalty for the optimization function is as follows:

$$J_1 = \sum_{i=1}^{N_p} \|\mathbf{e}\left(i|t\right)\|_{\mathbf{P}}^2 \tag{18}$$

where $\mathbf{P}$ is the weight matrix.

Path tracking control also needs to ensure that the wheeled mobile robot travels as smoothly as possible, so the second penalty is as follows:

$$J_2 = \sum_{i=1}^{N_p} \|\Delta\mathbf{u}\left(i|t\right)\|_{\mathbf{Q}}^2 \tag{19}$$

where:

$$\Delta\mathbf{u}\left(i|t\right) = \mathbf{u}\left(i|t\right) - \mathbf{u}\left(i-1|t\right) \tag{20}$$

and $\mathbf{Q}$ is the weight matrix.

In addition, in order to ensure that the wheeled mobile robot can travel in a straight line under slight disturbance, the third penalty item is designed as follows:

$$J_3 = \sum_{i=1}^{N_p} \|\omega\left(i|t\right)\|_{\mathbf{R}}^2 \tag{21}$$

where $\mathbf{R}$ is the weight matrix.

Finally, the optimization function is:

$$J = J_1 + J_2 + J_3 \tag{22}$$

Therefore, the path tracking control based on MPC is equivalent to solving the following quadratic optimization problem:

$$\begin{aligned}\min_{\mathbf{e},\Delta\mathbf{u},\omega} J &= \sum_{i=1}^{N_p} \|\mathbf{e}\left(i|t\right)\|_{\mathbf{P}}^2\\ &\quad + \sum_{i=1}^{N_p} \|\Delta\mathbf{u}\left(i|t\right)\|_{\mathbf{Q}}^2\\ &\quad + \sum_{i=1}^{N_p} \|\omega\left(i|t\right)\|_{\mathbf{R}}^2\\ s.t.\ \Delta v &\in \left(\Delta v_{\min}, \Delta v_{\max}\right)\\ \Delta\omega &\in \left(\Delta\omega_{\min}, \Delta\omega_{\max}\right)\end{aligned} \tag{23}$$

The above formula can be solved by a variety of optimization algorithms. In this paper, the fmincon function in MATLAB is used.

In the control sequence (24) obtained by solving (23), the first value is the output of the MPC controller.

$$\mathbf{U} = \left[\begin{array}{ccc}\mathbf{u}\left(1|t\right) & \cdots & \mathbf{u}\left(N_p|t\right)\end{array}\right]^T \tag{24}$$

B. SIMULATION

The MPC controller is verified by MATLAB/Simulink and ADAMS. Fig.4 shows the ADAMS model of the wheeled mobile robot. Since this model presents position state information directly, the positioning system and the sensing system are not included in the simulation system.

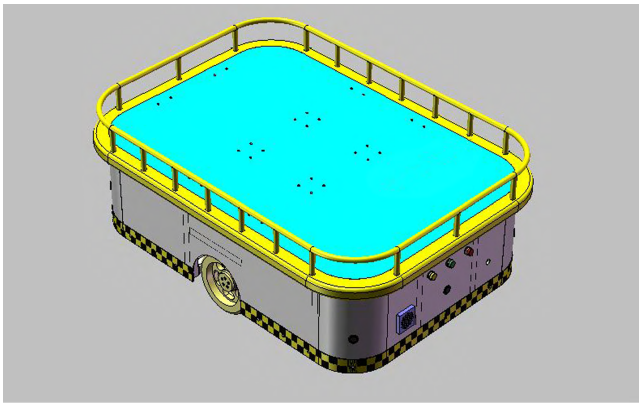

FIGURE 4. ADAMS model of the wheeled mobile robot.

In the simulation, the proposed path tracking controller based on dynamic prediction model is compared to the controller based on the kinematics prediction model. The penalty terms of these two controllers are the same, and the parameters are shown in Table 2. And v_{xref} is the reference of the longitudinal velocity. Its function is to obtain reference points on the given path. As shown in Fig.5, A_0 is the closest point to the geometric center of the robot on the reference path, then $A_i, i = 0, 1, \cdots, N_p$ are selected as the reference points on the given path, and the arc length between every two points is equal to Tv_{xref}.

TABLE 2. Parameters in MPC controllers.

Symbol	MPC-Dynamic	MPC-Kinematics
v_{xref}	5m/s	5m/s
N_p	10	10
$\mathbf{P}$	$\begin{bmatrix}100 & 0 & 0 & 0\\ 0 & 100 & 0 & 0\\ 0 & 0 & 100 & 0\\ 0 & 0 & 0 & 0\end{bmatrix}$	$\begin{bmatrix}100 & 0 & 0\\ 0 & 100 & 0\\ 0 & 0 & 100\end{bmatrix}$
$\mathbf{Q}$	$\begin{bmatrix}1 & 0\\ 0 & 1\end{bmatrix}$	$\begin{bmatrix}1 & 0\\ 0 & 1\end{bmatrix}$
$\mathbf{R}$	1	1

In the simulation results, in order to display the position error decomposed into the X and Y directions more clearly, the displacement error is defined as shown in Fig.6.

On the given path, A_0 is the closest point to the geometric center P of the robot. P_1P_2 is the tangent of the given path at

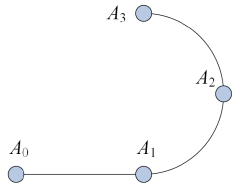

FIGURE 5. The reference point on the given path.

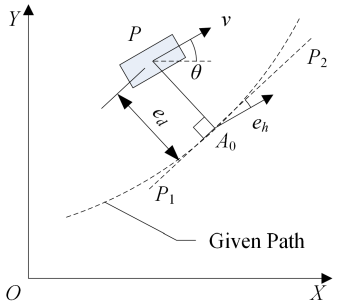

FIGURE 6. The definition of the errors.

point P_0. The displacement error e_d is the length of PP_0. The heading error e_h is the difference between the heading of the robot and the heading of the given path at point P_0.

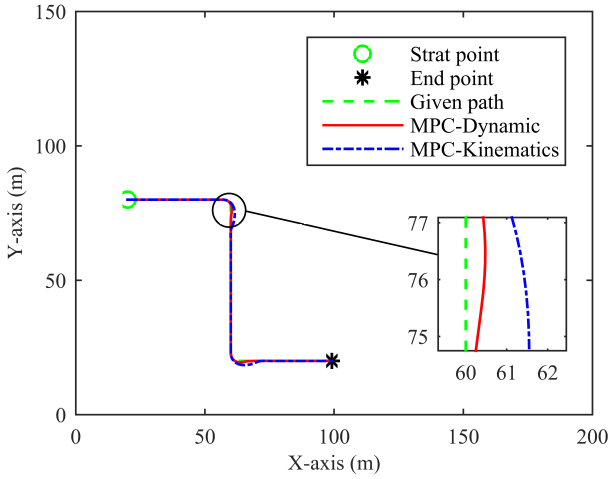

FIGURE 7. The trajectory of the dynamic-based MPC controller and the kinematics-based MPC controller.

Fig.7 shows the trajectory of the dynamic-based MPC controller and the kinematics-based MPC controller. The given path is composed of straight lines and arcs, and the radius of the arc is 2.5m. As can be seen from the partial enlargement, the dynamic-based MPC controller makes the trajectory of the wheeled mobile robot closer to the given path than that of the kinematics-based MPC controller.

Fig.8 shows the longitudinal velocity and Fig.9 shows the heading angle speed. The reason why the longitudinal velocity increases during the course of steering is that there is a coupling relationship between the reference point coordinates and the longitudinal velocity. As shown in Fig.10, $B_i, i = 0, 1, 2, 3$ and $B_i', i = 0, 1, 2, 3$ are two different sets of predicted poses. Since the robot is affected by the lateral forces in the steering process, the high longitudinal velocity

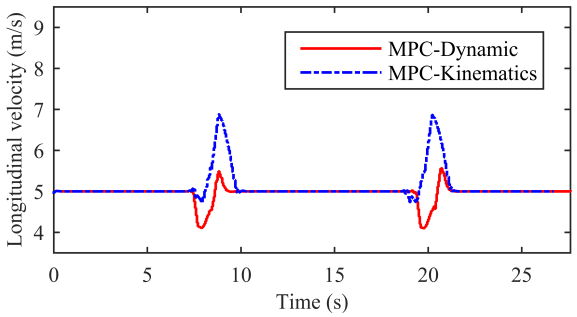

FIGURE 8. The longitudinal velocity of the dynamic-based MPC controller and the kinematics-based MPC controller.

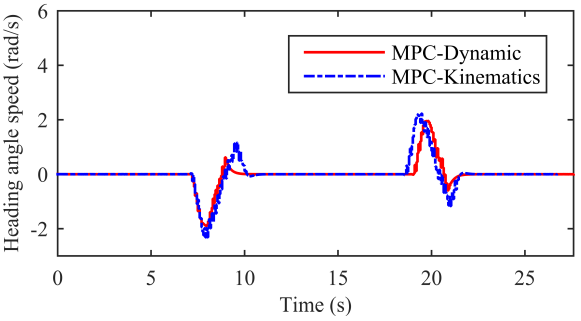

FIGURE 9. The heading angle speed of the dynamic-based MPC controller and the kinematics-based MPC controller.

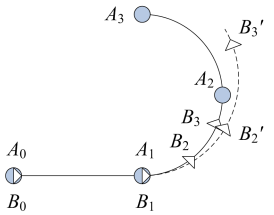

FIGURE 10. The coupling relationship between the reference path coordinates and the longitudinal velocity.

results to the large turning radius. But B_2' is closer to A_2 than B_2, and B_3' is closer to A_3 than B_3, so the MPC controller will control the robot to travel along $B_i', i = 0, 1, 2, 3$ at higher longitudinal velocity rather than $B_i, i = 0, 1, 2, 3$ with less displacement errors.

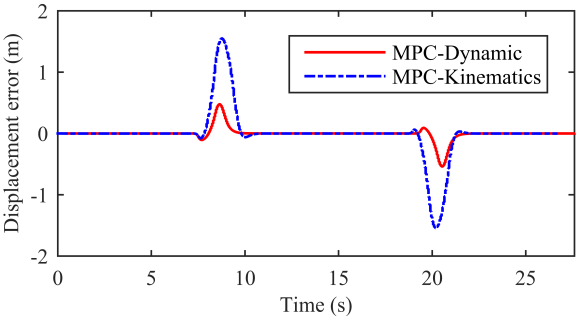

FIGURE 11. The displacement error of the dynamic-based MPC controller and the kinematics-based MPC controller.

Fig.11, Fig.12, Fig.13, Fig.14, and Fig.15 show the displacement error, heading error, lateral velocity, slip angle,

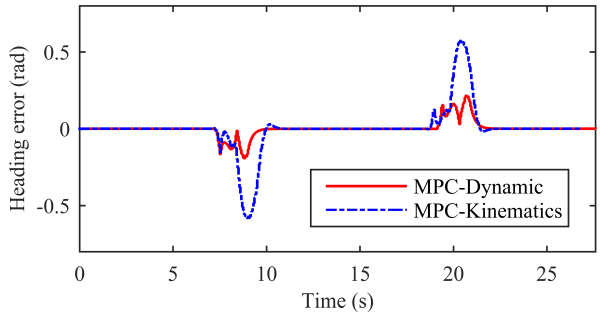

FIGURE 12. The heading error of the dynamic-based MPC controller and the kinematics-based MPC controller.

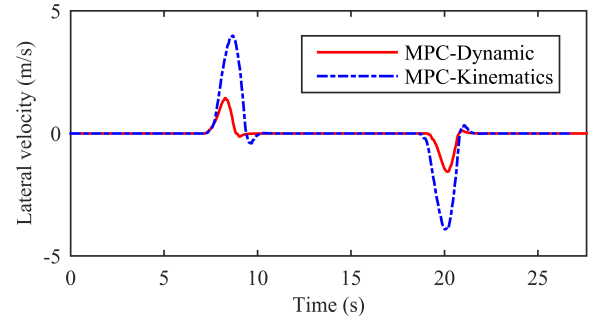

FIGURE 13. The lateral velocity of the dynamic-based MPC controller and the kinematics-based MPC controller.

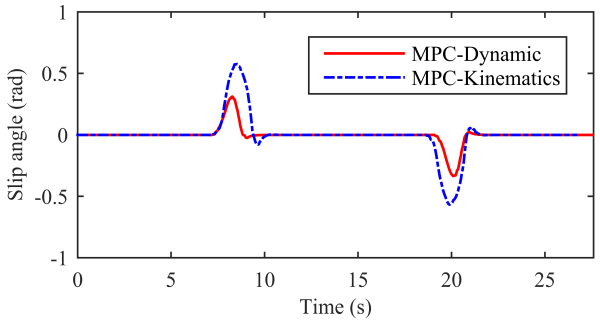

FIGURE 14. The slip angle of the dynamic-based MPC controller and the kinematics-based MPC controller.

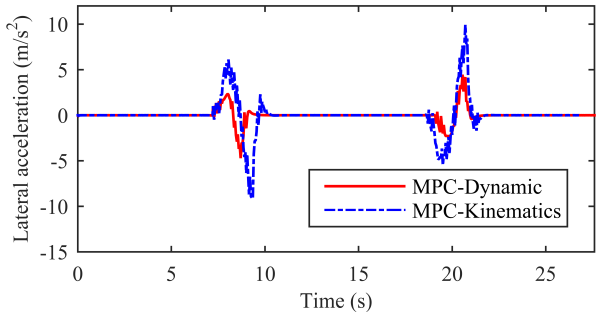

FIGURE 15. The lateral acceleration of the dynamic-based MPC controller and the kinematics-based MPC controller.

and lateral acceleration, respectively. The maximum value of these parameters is shown in Table 3.

The above results show that the dynamic-based MPC controller has higher control accuracy than the kinematics-based MPC controller. However, the maximum lateral velocity and the maximum sliding angle of the wheeled mobile robot under the control of the dynamic-based MPC controller are still large. Therefore, in order to solve this problem, the controller is improved in section IV.

TABLE 3. Maximum value of the dynamic-based MPC controller and the kinematics-based MPC controller.

Maximum value	MPC-Dynamic	MPC-Kinematics
Displacement error	0.5398m	1.5505m
Heading error	0.2154rad	0.5799rad
Lateral velocity	1.5667m/s	3.9886m/s
Slip angle	0.3369rad	0.5774rad
Lateral acceleration	4.7157m/s^2	9.9224m/s^2

IV. IMPROVEMENT AND SIMULATION OF MPC CONTROLLER

In order to further reduce the lateral acceleration, the lateral velocity, and the slip angle, the lateral velocity penalty term is added in the controller. In other words, set the weight matrix **P** as follows:

$$\mathbf{P} = \begin{bmatrix} 100 & 0 & 0 & 0 \\ 0 & 100 & 0 & 0 \\ 0 & 0 & 100 & 0 \\ 0 & 0 & 0 & 1000 \end{bmatrix} \tag{25}$$

This improved controller is named MPC-Dynamic 2. The other parameters of this controller are the same as those of the dynamic-based MPC controller in section III.

On the basis of MPC-Dynamic 2, in order to solve the problem mentioned in Fig.10, set the reference of the longitudinal velocity as follows:

$$v'_{xref} = \begin{cases} v_{xref}, & |\omega| > \omega_0 \\ v_x, & |\omega| \le \omega_0 \end{cases} \tag{26}$$

where ω_0 is a small value greater than zero.

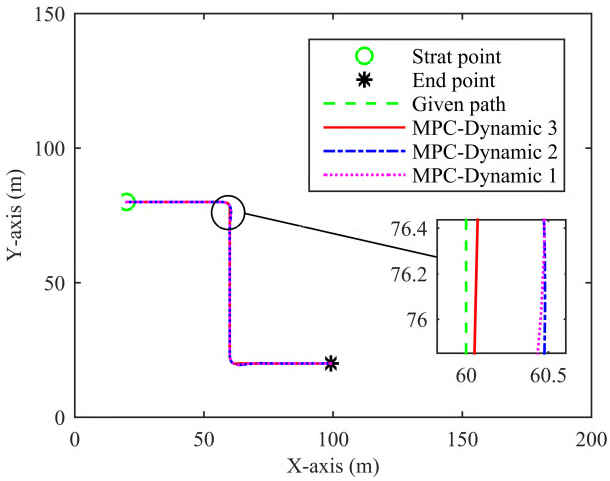

FIGURE 16. The trajectory of the improved controllers and the original controller.

This improved controller is named MPC-Dynamic 3. In this section, the dynamic-based MPC controller in

section III is named MPC-Dynamic 1, and is used to compare with MPC-Dynamic 2 and MPC-Dynamic 3.

A. COMPARISON OF THE IMPROVED CONTROLLERS WITH THE ORIGINAL CONTROLLER

Fig.16 shows the trajectory of the improved controllers and the original controller. The given path is the same as that in section III. As can be seen from the partial enlargement, the final improved MPC-Dynamic 3 makes the trajectory of the wheeled mobile robot closer to the reference path than MPC-Dynamic 2 and MPC-Dynamic 1.

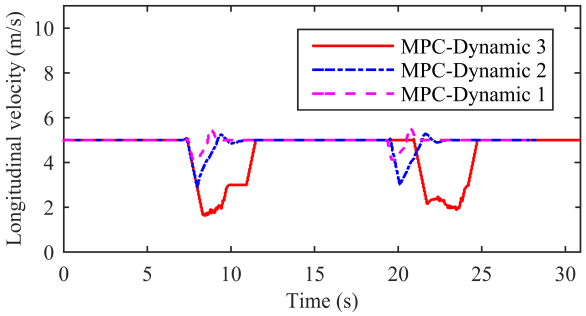

FIGURE 17. The longitudinal velocity of the improved controllers and the original controller.

Fig.17 shows the longitudinal velocity. During the course of steering, MPC-Dynamic 3 has the largest reduction of the longitudinal velocity, followed by MPC-Dynamic 2, and MPC-Dynamic 1 has the smallest reduction.

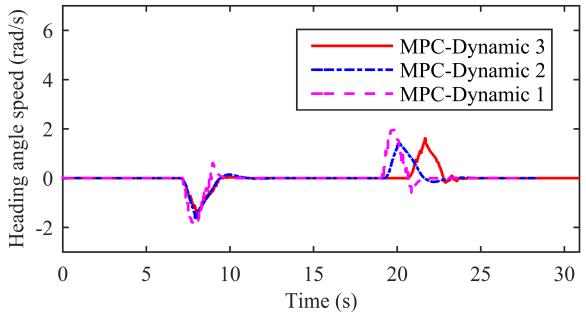

FIGURE 18. The heading angle speed of the improved controllers and the original controller.

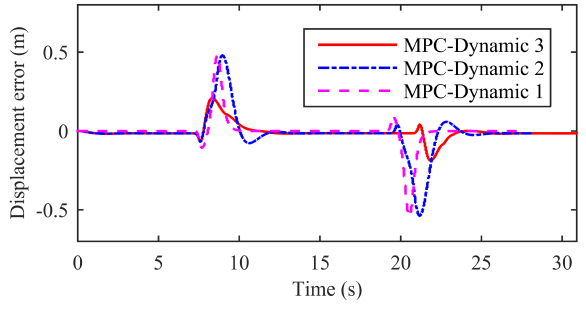

FIGURE 19. The displacement error of the improved controllers and the original controller.

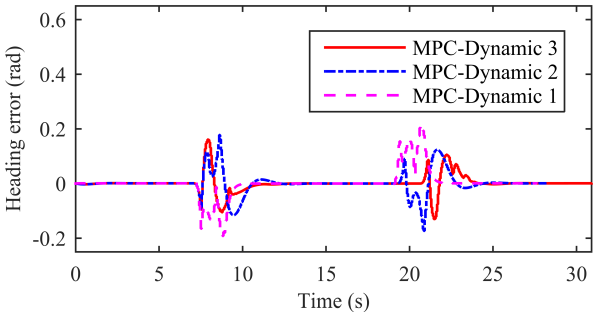

FIGURE 20. The heading error of the improved controllers and the original controller.

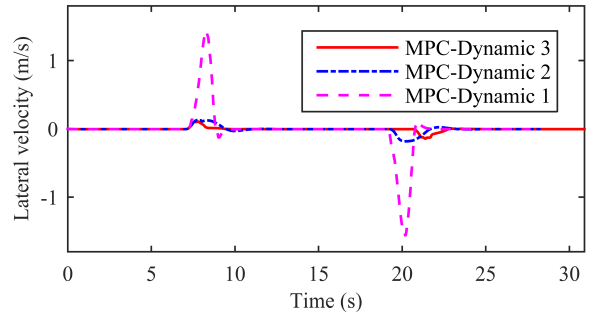

FIGURE 21. The lateral velocity of the improved controllers and the original controller.

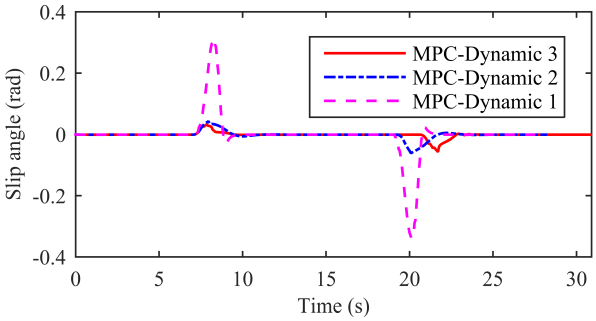

FIGURE 22. The slip angle of the improved controllers and the original controller.

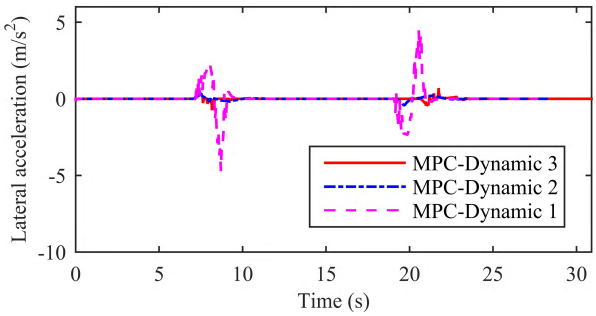

FIGURE 23. The lateral acceleration of the improved controllers and the original controller.

Fig.18 shows the heading angle speed. Fig.19, Fig.20, Fig.21, Fig.22, and Fig.23 show the displacement error, heading error, lateral velocity, slip angle, and lateral acceleration, respectively. The maximum value of these parameters is shown in Table 4.

TABLE 4. Maximum value of the controllers.

Maximum value	MPC-Dynamic 3	MPC-Dynamic 2	MPC-Dynamic 1	MPC-Kinematics
Displacement error	0.2086m	0.5376m	0.5398m	1.5505m
Heading error	0.1609rad	0.1776rad	0.2154rad	0.5799rad
Lateral velocity	0.1474m/s	0.1855m/s	1.5667m/s	3.9886m/s
Slip angle	0.0576rad	0.0617rad	0.3369rad	0.5774rad
Lateral acceleration	0.7478m/s^2	0.4162m/s^2	4.7157m/s^2	9.9224m/s^2

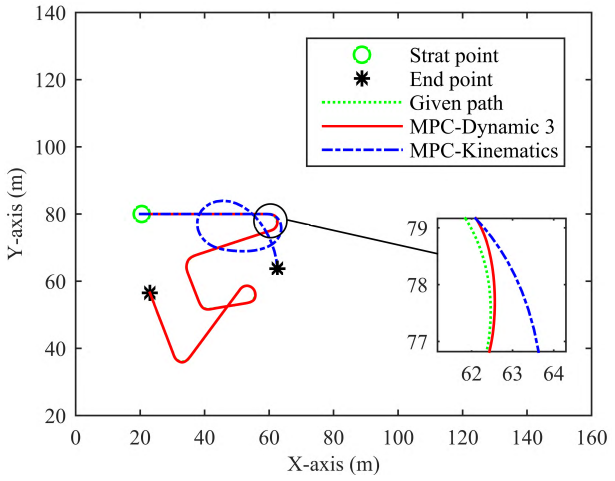

FIGURE 24. The trajectory of the simulation of the complex given path.

The above data shows that after adding the lateral velocity penalty term, the lateral velocity, lateral acceleration and slip angle of the wheeled mobile robot are greatly reduced, and the maximum slip angle is within the linear range of the tire [29]–[33], but the reduction of the maximum displacement error and the maximum heading error is small.

After adding the lateral velocity penalty term and decoupling the relationship between the longitudinal velocity and the reference point coordinates, the controller shows better performance. Compared to the kinematics-based MPC controller, the final improved dynamics-based MPC controller reduces the maximum displacement error by 86.55%, the maximum heading error by 72.25%, the maximum lateral velocity by 96.30%, the maximum sideslip angle by 90.02% and the maximum lateral acceleration by 92.46%.

B. SIMULATION OF THE COMPLEX GIVEN PATH

In order to further compare the dynamic-based MPC controller with the kinematics-based MPC controller, the given path is set to a complex path in this part of the simulation. The minimum radius of this path is 2.4691m. Fig.24 shows the trajectory.

Fig.25 shows the longitudinal velocity. Since the kinematics-based MPC controller cannot incorporate the lateral velocity penalty term, it cannot be improved like the dynamics-based MPC controller. Thus, when the error becomes large, the longitudinal velocity of the

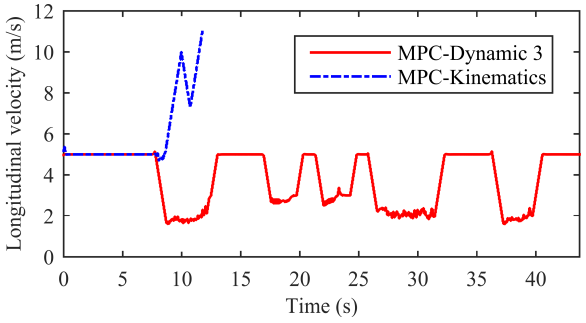

FIGURE 25. The longitudinal velocity of the simulation of the complex given path.

kinematics-based MPC controller increases and the performance of the controller is further deteriorated. Fig.26 shows the heading angle speed.

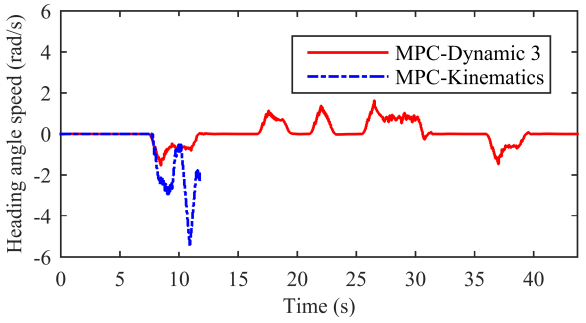

FIGURE 26. The heading angle speed of the simulation of the complex given path.

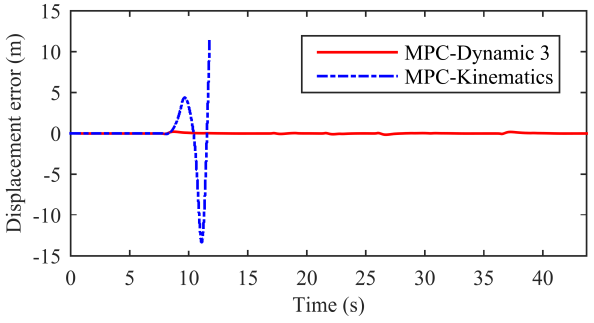

FIGURE 27. The displacement error of the simulation of the complex given path.

Fig.27, Fig.28, Fig.29, Fig.30, and Fig.31 show the displacement error, heading error, lateral velocity, slip angle, and lateral acceleration, respectively. The above parameters of the kinematics-based MPC controller are divergent. The maximum value of the dynamic-based MPC controller is shown in Table 5.

TABLE 5. Maximum value of MPC-Dynamic 3.

Displacement error	Heading error	Lateral velocity	Slip angle	Lateral acceleration
0.2043m	0.1063rad	0.1431m/s	0.0557rad	0.6934 m/s^2

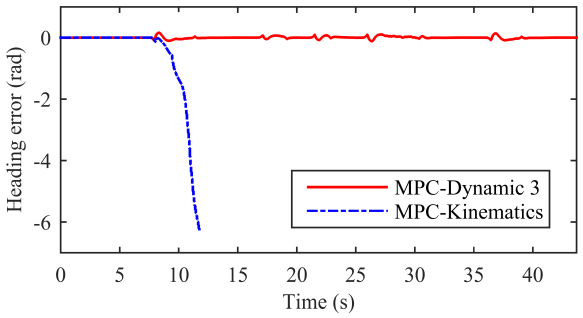

FIGURE 28. The heading error of the simulation of the complex given path.

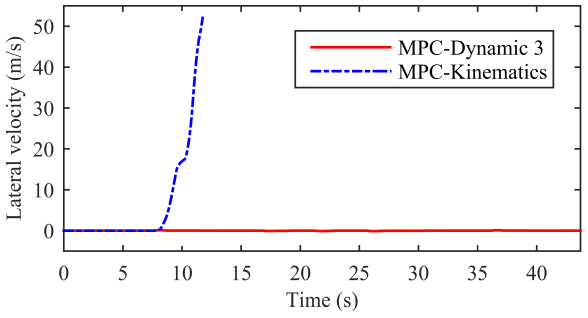

FIGURE 29. The lateral velocity of the simulation of the complex given path.

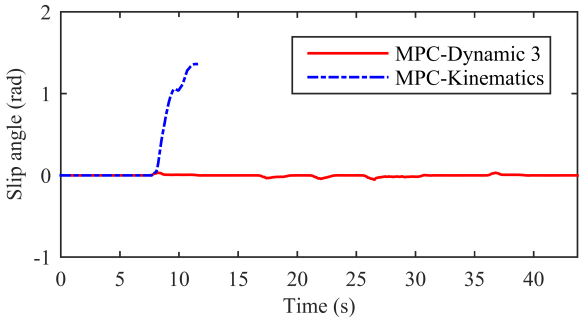

FIGURE 30. The slip angle of the simulation of the complex given path.

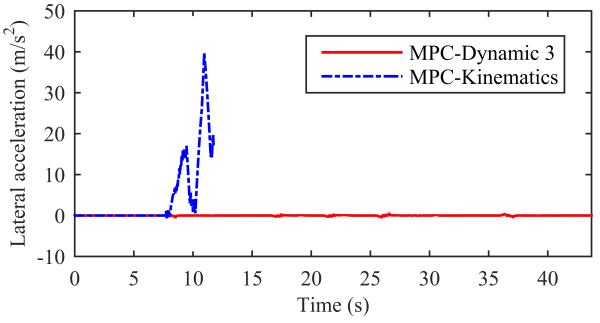

FIGURE 31. The lateral acceleration of the simulation of the complex given path.

C. DISTURBANCE SIMULATION

In order to simulate the error of the positioning system, we added the disturbance that is no more than 0.1m to X and Y, added the disturbance that is no more than 0.0175rad to θ. In order to simulate the sensor error, we added a disturbance

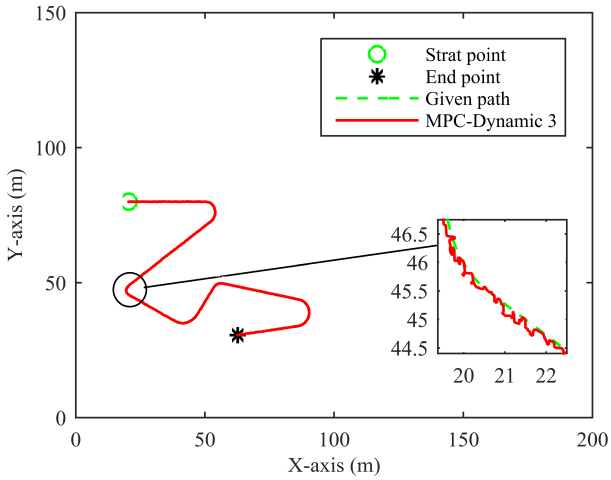

FIGURE 32. The trajectory of the disturbance simulation.

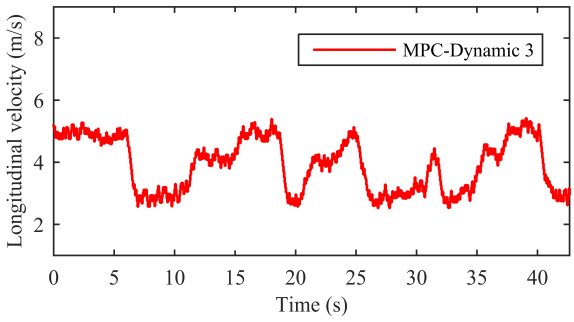

FIGURE 33. The longitudinal velocity of the disturbance simulation.

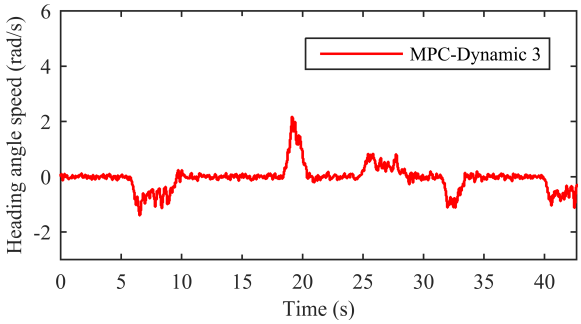

FIGURE 34. The heading angle speed of the disturbance simulation.

that is no more than 0.01m/s to v_y. Fig.32 shows the trajectory. Fig.33 shows the longitudinal velocity. Fig.34 presents the heading angle speed.

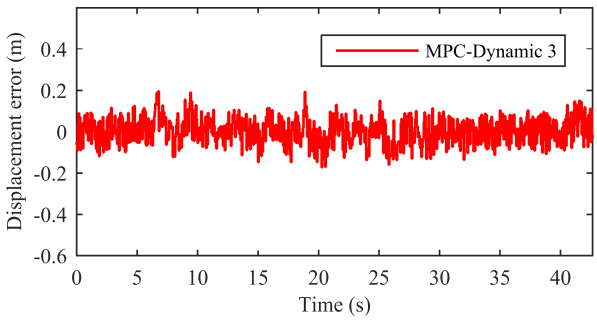

FIGURE 35. The displacement error of the disturbance simulation.

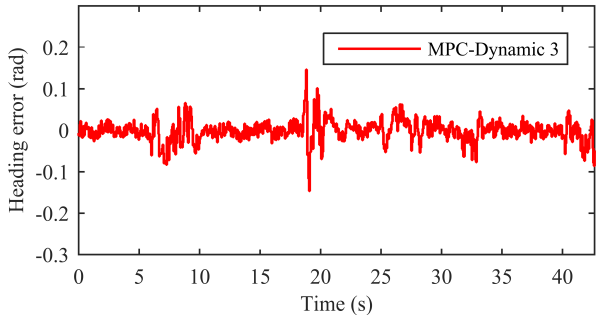

FIGURE 36. The heading error of the disturbance simulation.

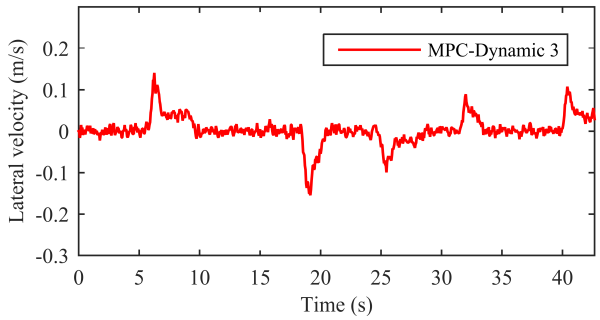

FIGURE 37. The lateral velocity of the disturbance simulation.

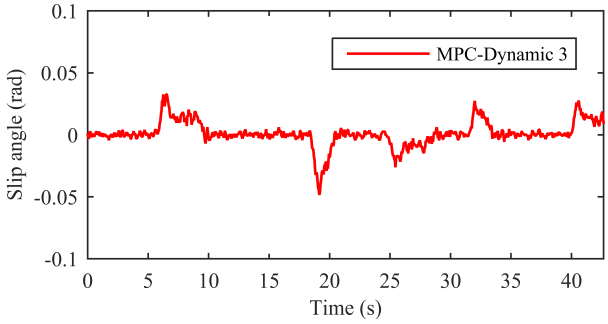

FIGURE 38. The slip angle of the disturbance simulation.

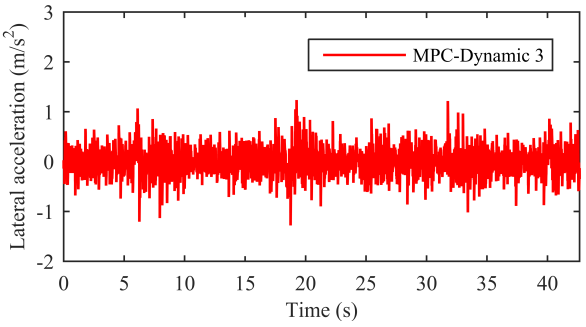

FIGURE 39. The lateral acceleration of the disturbance simulation.

Fig.35, Fig.36, Fig.37, Fig.38, and Fig.39 show the displacement error, heading error, lateral velocity, slip angle, and lateral acceleration, respectively. The maximum value of the dynamic-based MPC controller is shown in Table 6.

TABLE 6. Maximum value of disturbance simulation.

Displacement error	Heading error	Lateral velocity	Slip angle	Lateral acceleration
0.1963m	0.1464rad	0.1546m/s	0.0485rad	1.2803 m/s^2

V. CONCLUSION

In order to improve the operating efficiency of the wheeled mobile robot, we introduced the tire mechanics and proposed a path tracking controller based on the dynamic prediction model. The controller is verified by simulation and the following conclusions can be obtained.

First, when the penalty terms are the same, the dynamic-based MPC controller is more accurate than the kinematics-based MPC controller. However, in this case, the wheeled mobile robot still has a large lateral velocity when steering, and the maximum slip angle is 0.3369rad, which is larger than the upper limit of the linear range of the tire lateral force.

Second, the dynamic-based MPC controller can be improved by adding the lateral velocity penalty term, but the kinematics-based MPC controllers cannot. After adding the lateral velocity penalty term and optimizing the reference point selection method, the performance of the improved dynamic-based MPC controller is more excellent compared to that of the kinematics-based MPC controller. The maximum values of displacement error, heading error, lateral velocity and slip angle were reduced by 86.55%, 72.25%, 96.30%, and 90.02%, respectively.

Third, the kinematics-based MPC controller fails to track the complex given path, while the performance of the improved dynamic-based MPC controller to track the complex given path is as good as its performance when tracking the simply given path. In all simulations of this paper, the maximum values of displacement error, heading error, lateral velocity, and slip angle of the improved dynamic-based MPC controller are 0.2086m, 0.1609rad, 0.1546m/s, and 0.0576rad, respectively. The maximum slip angle is within the linear range of the tire lateral force [30]. Thus, the safety of the wheeled mobile robot can be guaranteed.

From the aspect of theory, we improved the MPC-based path tracking control method of mobile robots with the help of tire mechanics. In the terms of the application, we improved the safety of mobile robots at the high longitudinal velocity. In a word, we firmly believe that the proposed controller is helpful to improve the performance of the path tracking of wheeled mobile robots.

APPENDIX

A. KINEMATICS MODEL OF THE WHEELED MOBILE ROBOT

$$\begin{cases} \dot{X} = v_x \cos\theta \\ \dot{Y} = v_x \sin\theta \\ \dot{\theta} = \omega \end{cases} \tag{27}$$

B. MAGIC FORMULA

Magic Formula is a mature formula in the field of vehicle engineering. In this paper, Magic Formula is quoted from [29]–[33], so this formula is not deduced here.

In this paper, we refer to two aspects of Magic Formula: lateral force and longitudinal force.

The expression of the lateral force of the Magic Formula proposed by Pacejka is:

$$F_y = C \sin(D) + S_v \tag{28}$$

where:

$$\begin{cases} C = C_1 \\ D = C_2 \arctan(E) \\ E = C_3 x - C_4 (C_3 x - \arctan(C_3 x)) \\ x = \alpha + S_h \\ C_1 = A_0 F_z^2 + A_1 F_z \\ C_2 = A_2 \\ C_3 = \dfrac{A_3 \sin\left(2 \arctan \dfrac{F_z}{A_4}\right)}{C_1 C_2} \\ C_4 = A_5 F + A_6 \\ S_h = A_7 F_z + A_8 \\ S_v = A_9 F_z + A_{10} \end{cases} \tag{29}$$

where F_z is the vertical load on one tire, and $F_z = 3$kN in this paper.

The expression of the longitudinal force of the Magic Formula proposed by Pacejka is:

$$F_x = C \sin(D) + S_v \tag{30}$$

where:

$$\begin{cases} C = C_1 \\ D = C_2 \arctan(E) \\ E = C_3 x - C_4 (C_3 x - \arctan(C_3 x)) \\ x = s + S_h \\ C_1 = B_0 F_z^2 + B_1 F_z \\ C_2 = B_2 \\ C_3 = \dfrac{\left(B_3 F_z^2 + B_4 F_z\right) e^{-B_5 F_z}}{C_1 C_2} \\ C_4 = B_6 F_z^2 + B_7 F + B_8 \\ S_h = B_9 F_z + B_{10} \\ S_v = 0 \end{cases} \tag{31}$$

where s is the longitudinal slip ratio.

The parameters for Magic Formula come from the tire supplier, as shown in Table 7.

TABLE 7. Parameters for magic formula.

Parameter	Value	Parameter	Value
A_0	-34	B_0	-9.46
A_1	1250	B_1	1490
A_2	-1.65	B_2	2.37272
A_3	3036	B_3	130
A_4	12.8	B_4	276
A_5	-0.02103	B_5	0.0886
A_6	0.77394	B_6	0.00402
A_7	0.013442	B_7	0.0615
A_8	0.003709	B_8	1.2
A_9	1.21356	B_9	0.0299
A_{10}	6.26206	B_{10}	-0.176

REFERENCES

[1] M. Baratta, G. Genta, D. Laurenzano, and D. Misul, "Exploring the surface of the Moon and Mars: What kind of ground vehicles are required?" *Acta Astronautica*, vol. 154, pp. 204–213, Jan. 2018. doi: 10.1016/j.actaastro.2018.04.030.

[2] Z. J. Jia, Y. D. Song, and W. C. Cai, "Bio-inspired approach for smooth motion control of wheeled mobile robots," *Cogn. Comput.*, vol. 5, no. 2, pp. 252–263, Jun. 2013. doi: 10.1007/s12559-012-9186-8.

[3] T. Takei, R. Imamura, and S. Yuta, "Baggage transportation and navigation by a wheeled inverted pendulum mobile robot," *IEEE Trans. Ind. Electron.*, vol. 56, no. 10, pp. 3985–3994, Oct. 2009. doi: 10.1109/TIE.2009.2027252.

[4] N. Sidek and N. Sarkar, "Dynamic modeling and control of nonholonomic mobile robot with lateral slip," in *Proc. 3rd Int. Conf. Syst. (ICONS)*, Cancun, Mexico, Apr. 2008, pp. 35–40. doi: 10.1109/ICONS.2008.22.

[5] K. Shojaei and A. M. Shahri, "Output feedback tracking control of uncertain non-holonomic wheeled mobile robots: A dynamic surface control approach," *IET Control Theory Appl.*, vol. 6, no. 2, pp. 216–228, Jan. 2012. doi: 10.1049/iet-cta.2011.0169.

[6] J. Chang and Q. Meng, "Trajectory tracking control of nonholonomic wheeled mobile robots," in *Proc. IEEE Int. Conf. Inf. Automat. (ICIA)*, Harbin, China, Jun. 2010, pp. 688–692. doi: 10.1109/ICINFA.2010.5512422.

[7] T. Szepe and S. Assal, "Pure pursuit trajectory tracking approach: Comparison and experimental validation," *Int. J. Robot. Automat.*, vol. 27, no. 4, pp. 355–363, Jan. 2012. doi: 10.2316./Journal.206.2012.4.206-3606.

[8] I. Zohar, A. Ailon, and R. Rabinovici, "Mobile robot characterized by dynamic and kinematic equations and actuator dynamics: Trajectory tracking and related application," *Robot. Auton. Syst.*, vol. 59, no. 6, pp. 343–353, Jun. 2011. doi: 10.1016/j.robot.2010.12.001.

[9] L. Zuo, X. Xu, C. Liu, and Z. Huang, "A hierarchical reinforcement learning approach for optimal path tracking of wheeled mobile robots," *Neural Comput. Appl.*, vol. 23, nos. 7–8, pp. 1873–1883, Dec. 2013. doi: 10.1007/s00521-012-1243-4.

[10] S. T. Mitrović and Ž. M. ÃŘurović, "Fuzzy logic controller for bidirectional garaging of a differential drive mobile robot," *Adv. Robot.*, vol. 24, nos. 8–9, pp. 1291–1311, Apr. 2010. doi: 10.1163/016918610X501444.

[11] R.-J. Wai and C.-M. Liu, "Design of dynamic petri recurrent fuzzy neural network and its application to path-tracking control of nonholonomic mobile robot," *IEEE Trans. Ind. Electron.*, vol. 56, no. 7, pp. 2667–2683, Jul. 2009. doi: 10.1109/TIE.2009.2020077.

[12] J.-X. Xu, Z.-Q. Guo, and T. H. Tong, "Design and implementation of integral sliding-mode control on an underactuated two-wheeled mobile robot," *IEEE Trans. Ind. Electron.*, vol. 61, no. 7, pp. 3671–3681, Jul. 2014. doi: 10.1109/TIE.2013.2282594.

[13] S. Roy, S. Nandy, R. Ray, and S. N. Shome, "Robust path tracking control of nonholonomic wheeled mobile robot: Experimental validation," *Int. J. Control Autom. Syst.*, vol. 13, no. 4, pp. 897–905, 2015. doi: 10.1007/s12555-014-0178-1.

[14] J. Huang, C. Wen, W. Wang, and Z.-P. Jiang, "Adaptive stabilization and tracking control of a nonholonomic mobile robot with input saturation and disturbance," *Syst. Control Lett.*, vol. 62, no. 3, pp. 234–241, Mar. 2013. doi: 10.1016/j.sysconle.2012.11.020.

[15] J.-Y. Zhai and Z.-B. Song, "Adaptive sliding mode trajectory tracking control for wheeled mobile robots," *Int. J. Control*, Feb. 2018. Accessed: Feb. 5, 2018. doi: 10.1080/00207179.2018.1436194.

[16] Z. Li, C. Yang, C. Su, J. Deng, and W. Zhang, "Vision-based model predictive control for steering of a nonholonomic mobile robot," *IEEE Trans. Control Syst. Technol.*, vol. 24, no. 2, pp. 553–564, Mar. 2015. doi: 10.1109/TCST.2015.2454484.

[17] Z. Li, J. Deng, R. Lu, Y. Xu, J. Bai, and C. Su, "Trajectory-tracking control of mobile robot systems incorporating neural-dynamic optimized model predictive approach," *IEEE Trans. Syst., Man, Cybern. Syst.*, vol. 46, no. 6, pp. 740–749, Jun. 2016. doi: 10.1109/TSMC.2015.2465352.

[18] T. P. Nascimento, C. E. Dórea, and L. M. G. Gonçalves, "Nonholonomic mobile robots' trajectory tracking model predictive control: A survey," *Robotica*, vol. 36, no. 5, pp. 676–696, May 2018. doi: 10.1017/S0263574717000637.

[19] T. P. Nascimento, C. E. T. Dórea, and L. M. G. Gonçalves, "Nonlinear model predictive control for trajectory tracking of nonholonomic mobile robots: A modified approach," *Int. J. Adv. Robotic Syst.*, vol. 15, no. 1, Feb. 2018, Art. no. 1729881418760461. Accessed on: Jan. 29, 2018. doi: 10.1177/1729881418760461.

[20] G. Franzé and W. Lucia, "An obstacle avoidance model predictive control scheme for mobile robots subject to nonholonomic constraints: A sum-of-squares approach," *J. Franklin Inst.*, vol. 352, no. 6, pp. 2358–2380, Jun. 2015. doi: 10.1016/j.jfranklin.2015.03.021.

[21] M. H. Amoozgar and Y. M. Zhang, "Trajectory tracking of wheeled mobile robots: A kinematical approach," in *Proc. IEEE/ASME Int. Conf. Mechatronic Embedded Syst. Appl.*, Suzhou, China, Jul. 2012, pp. 275–280. doi: 10.1109/MESA.2012.6275574.

[22] K. Kanjanawanishkul, M. Hofmeister, and A. Zell, "Smooth reference tracking of a mobile robot using nonlinear model predictive control," in *Proc. ECMR, Mlini/Dubrovnik, Croatia*, Sep. 2009, pp. 161–166.

[23] L. Pacheco and N. Luo, "Experiences with online local model predictive control for WMR navigation," in *Proc. IEEE 11th Int. Conf. Control Automat. Robot. Vis. (ICARCV)*, Singapore, Dec. 2010, pp. 370–377. doi: 10.1109/ICARCV.2010.5707226.

[24] J. M. Maciejowski, "Introduction," in *Predictive Control with Constraints*, New York, NY, USA: Pearson, 2002, pp. 1–6.

[25] J. A. Riul, A. G. C. Junior, and P. H. M. Montenegro, "Nonlinear neural model of a robot five degrees of freedom," *IEEE Latin Amer. Trans.*, vol. 14, no. 4, pp. 1652–1655, Apr. 2016. doi: 10.1109/TLA.2016.7483496.

[26] J. A. Monroy, E. Campos, and J. A. Torres, "Attitude control of a micro AUV through an embedded system," *IEEE Latin Amer. Trans.*, vol. 15, no. 4, pp. 603–612, Apr. 2017. doi: 10.1109/TLA.2017.7896344.

[27] M. Roozegar, M. J. Mahjoob, and M. Ayati, "Adaptive tracking control of a nonholonomic pendulum-driven spherical robot by using a model-reference adaptive system," *J. Mech. Sci. Technol.*, vol. 32, no. 2, pp. 845–853, Feb. 2018. doi: 10.1007/s12206-018-0135-z.

[28] S. R. Sahoo and S. S. Chiddarwar, "Dynamic modelling of four wheel skid mobile robot by unified bond graph approach," in *Proc. Int. Conf. Robot., Current Trends Future Challenges (RCTFC)*, Thanjavur, India, Dec. 2016, pp. 1–6. doi: 10.1109/RCTFC.2016.7893412.

[29] S. Wei, K. Uthaichana, M. Žefran, and R. Decarlo, "Hybrid model predictive control for the stabilization of wheeled mobile robots subject to wheel slippage," *IEEE Trans. Control Syst. Technol.*, vol. 21, no. 6, pp. 2181–2193, Nov. 2013. doi: 10.1109/TCST.2012.2227964.

[30] J. Gong, Y. Jiang, and W. Xu, "2.2 Vehicle dynamics modeling and verification," in *Model Predictive Control Self-driving Vehicles*. Beijing, China: Beijing Institute of Technology Press, 2014, pp. 22–35.

[31] F. Farroni, R. Lamberti, N. Mancinelli, and F. Timpone, "TRIP-ID: A tool for a smart and interactive identification of Magic Formula tyre model parameters from experimental data acquired on track or test rig," *Mech. Syst. Signal Process.*, vol. 102, pp. 1–22, Mar. 2018. doi: 10.1016/j.ymssp.2017.07.025.

[32] J. A. Cabrera, J. J. Castillo, J. Pérez, J. Velasco, A. Guerra, and P. Hernández, "A procedure for determining tire-road friction characteristics using a modification of the magic formula based on experimental results," *Sensors*, vol. 18, no. 3, p. 896, Mar. 2018. doi: 10.3390/s18030896.

[33] C. Long and H. Chen, "Comparative study between the magic formula and the neural network tire model based on genetic algorithm," in *Proc. IEEE 3rd Int. Symp. Intell. Inf. Technol. Secur. Inform. (IITSI)*, Jinggangshan, China, Apr. 2010, pp. 280–284. doi: 10.1109/IITSI.2010.138.

GUOXING BAI received the B.Eng. degree in vehicle engineering from Northeastern University, Shenyang, China, in 2014. He is currently pursuing the Ph.D. degree in mechanical engineering with the University of Science and Technology Beijing, Beijing, China. His research interests include the path tracking control and model predictive control.

LI LIU received the Ph.D. degree in mechanical engineering from the University of Science and Technology Beijing, Beijing, China, in 2012, where he is currently a Professor with the School of Mechanical Engineering. His research interests include the control of driverless vehicles and intelligent transportation.

YU MENG received the M.S. and Ph.D. degrees in computer science and technology from Jilin University, Changchun, China, in 2007. He is currently an Associate Professor with the School of Mechanical Engineering, University of Science and Technology Beijing, Beijing, China. His research interests include computer vision and intelligent vehicle.

WEIDONG LUO received the M.S. degree in petroleum mechanical engineering from the China University of Petroleum, Beijing, China, in 1985. He is currently a Professor with the School of Mechanical Engineering, University of Science and Technology Beijing, Beijing. His research interests include mining machinery and petroleum mechanics.

QING GU received the Ph.D. degree in intelligent traffic engineering from Beijing Jiaotong University, Beijing, China, in 2014. She is currently an Assistant Professor with the School of Mechanical Engineering, University of Science and Technology Beijing, Beijing. Her research interests include systems modeling, control, and optimization with application in intelligent transportation systems.

JUNPENG WANG is currently pursuing the M.S. degree in mechanical engineering with the University of Science and Technology Beijing, Beijing, China. His research interests include the path tracking control for robots, model predictive control, and autonomous vehicles.